Paper no: 972

EFFECTS OF SPECIMEN ORIENTATION ON THE FATIGUE CRACK GROWTH RESISTANCE OF CROSS-PLY TI-6AL-4V/SCS-6 METAL-MATRIX COMPOSITES

A. Yasmin, T. J. A. Doel and P. Bowen

School of Metallurgy and Materials/IRC in Materials for High Performance Applications
The University of Birmingham, Edgbaston, Birmingham B15 2TT, UK

SUMMARY: The fatigue crack growth resistance of cross-ply $[0/90]_{2s}$ laminate of Ti-6Al-4V reinforced with continuous SCS-6 fibres has been investigated at room temperature for three different mode-I crack growth directions relative to the axis of the fibres in the $[0/90]_{2s}$ laminate: 30, 45, and 60°. The tests were conducted under three point bending at initial applied stress intensity range (ΔK_{ini}) from 8 to 14 MPa$\sqrt{m}$. When tested with the mode-I crack growth direction at 30 and 60° to the fibre axis, a CA/CF (Crack Arrest/Catastrophic Failure) transition of 10-12 MPa$\sqrt{m}$ was found, whereas when the mode-I crack growth direction was at 45° to the fibre axis the transition was 8-10 MPa$\sqrt{m}$. Unlike crack propagation in unidirectional composites for crack growth perpendicular to the fibre axis, and for crack growth perpendicular (and parallel) to the fibre axis in $[90/0]_{2s}$ and $[0/90]_{2s}$ cross-ply laminates, the fatigue crack is found to grow at an angle to the mode-I direction. For the specimens where mode-I directions are at 60 and 30° to the fibre axis, single dominant fatigue cracks were found to grow. However in the case of 45°, multiple cracks have been found to grow under some of the conditions used.

KEYWORDS: Effects of crack orientation, cross-ply, fatigue crack growth, fibre orientation, silicon carbide fibre, fibre bridging, crack arrest and catastrophic failure.

INTRODUCTION

The high specific strength and high specific stiffness to weight ratios of titanium based metal matrix composites (TMCs) make them potential materials for high temperature structural purposes, especially in the aerospace industry. However, the highly anisotropic properties of strength and stiffness primarily in the fibre direction of unidirectionally reinforced MMCs limit the utilisation of this type of composite if it is to be subjected to multiaxial stressing. Therefore one trend is to align reinforcement fibres or plies in different orientations to give cross-ply and angle-ply composites. This type of MMC can be used for highly stressed rotating parts operating at moderate to high temperatures [1].

As a new material for structural purposes, comprehensive investigations of damage tolerance behaviour of this type of composite are needed. To date, detailed studies have been carried out on unidirectional composites to determine, for example, their fatigue crack growth resistance [2-3] and effects of interfacial strength [4], fibre volume fraction [5] and stress-ratio [6]. Some studies have also been reported on cross-ply [7-10] and angle-ply [11-12] MMCs. However investigation of effect of lay-up sequence on damage mechanisms and fatigue behaviour requires further study. In a previous study [13], the effects of fibre orientation, fibre volume fraction and the stacking sequence on damage mechanisms and fatigue crack growth resistance have been illustrated for mode-I crack growth perpendicular (and parallel) to the $[0/90]_{2s}$ and $[90/0]_{2s}$ orientations of cross-ply Ti-6Al-4V/SCS-6 metal-matrix composites.

In the present study fatigue crack growth tests have been carried out on $[0/90]_{2s}$ cross-ply laminate with the mode-I crack growth direction at 30, 45 and 60° to the fibre axis, to determine the crack arrest/catastrophic failure (CA/CF) transition. In addition, the influence of the angles of the mode-I crack growth direction to the fibre axis on the fatigue mechanism of this laminate has also been outlined.

EXPERIMENTAL

The material studied in this research was the Ti-6Al-4V/SCS-6 metal-matrix composite. The composite is an 8-ply symmetrical laminate with a fibre volume fraction of 35%. The composite was supplied by Textron Speciality, USA as a plate where continuous silicon carbide fibres (SCS-6) of diameter of 140 μm were arranged in two directions $[\pm 90]$. This gives the possibility of $[0/90]_{2s}$ and $[90/0]_{2s}$ laminates.

Specimens with dimensions of 75 x 4 x 1.8 mm^3 were cut from the composite plate at angles of 30, 45 and 60° to the plate axis using electric discharge machining (EDM) which gives laminates with the first ply at 30, 45 and 60° to the mode-I crack growth direction respectively. The specimens were polished to a 1 μm diamond finish so that acetate replicas could be taken to observe the crack propagation during the testing with respect to the fibre axes (This has the disadvantage of damaging fibres at these surface positions and introduces additional complications into the interpretation of the fatigue crack growth resistance of these laminates). All initial specimens were notched using a diamond blade to a depth of approximately 0.5 mm, giving an approximate a_0/W ratio of 0.125, where a_0 is the initial notch depth and W is the test-piece width. All fatigue crack growth (FCG) tests were carried out in load control in an Instron 8501 Servohydraulic machine equipped with a 5 kN load cell.

Each FCG test was carried out at room temperature under three point bending conditions at a frequency of 10 Hz and a stress ratio, R of 0.1(where $R = \sigma_{min}/\sigma_{max}$ and σ_{min}, σ_{max} are the minimum and maximum stress applied over the fatigue cycle respectively). A constant span to width ratio (s/W) of 15:1 was maintained for all tests. Changes in crack length were monitored using the direct current potential difference (DCPD) technique. Acoustic emission was used to monitor *in situ* fibre failure during the tests.

Heat tinting was also carried out on crack arrested specimens for each orientation. This treatment was performed by placing the specimens in a furnace at 500 °C for 15 minutes. This treatment causes oxidation of the crack surfaces and gives it a coloured tint, which reveals the shape of the crack when the test was stopped.
After testing, polished metallographic sections were studied optically and the fracture surfaces were examined on an Hitachi S400 FEG scanning electron microscope at 20 kV and 45° tilt.

RESULTS AND DISCUSSION

The fatigue crack growth resistance curves, shown in terms of crack growth rate (da/dN) versus crack length (a) are shown for each orientation in figs. 1 and 2. Fig. 1 shows curves for an initial stress intensity range (ΔK_{ini}) of 12 MPa$\sqrt{m}$ and fig. 2 shows curves for an initial stress intensity range (ΔK_{ini}) of 10 MPa$\sqrt{m}$. The graphs show the variation of crack growth rate with crack length as a function of the angle of the mode-I crack growth direction with respect to the fibre axes. At ΔK_{ini} of 12 MPa$\sqrt{m}$, all three laminates show catastrophic failure. However, at ΔK_{ini} of 10 MPa$\sqrt{m}$, laminates with the mode-I crack growth direction at 30 and 60° to the fibre axes show crack arrest but the laminate with the mode-I crack growth direction at 45° still shows catastrophic failure. The laminate with the mode-I crack growth direction at 45° to the fibre axes shows crack arrest at ΔK_{ini} of 8 MPa$\sqrt{m}$. In this study, crack arrest has been defined as crack growth rate, da/dN ≤ 10^{-8} mm/cycle. Table 1 shows the number of cycles to failure for the specimens tested.

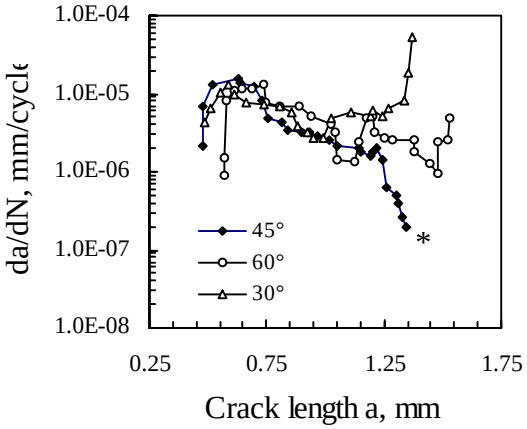

Fig. 1: da/dN versus crack length at ΔK_{ini} of 12 MPa$\sqrt{m}$.

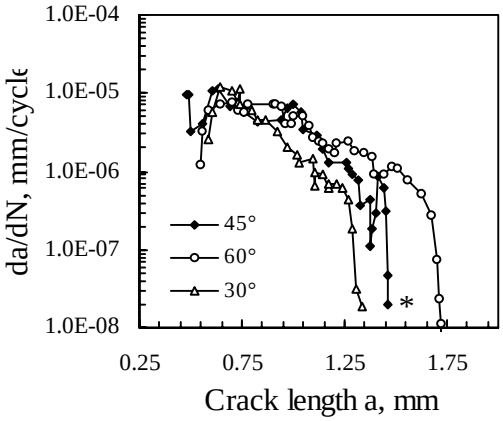

Fig. 2: da/dN versus crack length at ΔK_{ini} of 10 MPa$\sqrt{m}$.

The asterisk (*) in fig. 1 and 2 represents the point where the PD readings started to decrease i.e. the crack apparently becomes shorter. This was found to occur only for the laminate with the mode-I crack growth direction at 45° to the fibre axes. At ΔK_{ini} of 12 and 10 MPa$\sqrt{m}$, this happened after 440,000 and 910,000 cycles, which are 32 % and 56 % of the total lives respectively. It was found that this unusual behaviour occurred only when there were clearly visible secondary cracks outside of the PD monitoring wires, in addition to the primary crack that initiated from the notch and therefore the calibration becomes invalid. However such problems were not encountered with the laminates with mode-I crack growth directions at 30°and 60° to the fibre axes, both of which show the general behaviour of increasing PD with increasing crack length and no secondary cracks. Fig. 3 shows a micrograph of an acetate replica of the surface of a laminate with the mode-I crack growth direction at 45° to the fibre axes at ΔK_{ini} of 12 MPa$\sqrt{m}$ after 440,000 cycles, at which point the PD reading started to decrease. It can be seen that there are two secondary cracks (which are outside of the PD monitoring locations) in addition to the bifurcated primary crack.

Table 1: Fatigue crack growth tests at different mode-I crack growth directions of cross-ply Ti-6Al-4V/SCS-6 laminate (polished) at room temperature.

Mode-I crack direction	Notch length, mm	ΔK_{ini}, MPa$\sqrt{m}$	Total cycles	Result
± 45 to $0/90]_{2s}$	0.565	8	2,741,000	Crack arrest
	0.49	10	1,621,701	Catastrophic failure
	0.48	12	1,375,958	Catastrophic failure
	0.51	14	102,364	Catastrophic failure
	1.085	10	3,839,652	Crack arrest
	1.005	12	2,298,983	Catastrophic failure
60/30 to $[0/90]_{2s}$	0.55	10	2,085,000	Crack arrest
	0.57	12	319,694	Catastrophic failure
30/60 to $[0/90]_{2s}$	0.595	10	1,961,000	Crack arrest
	0.485	12	156,434	Catastrophic failure

The FCG test on the laminate with the mode-I crack growth direction at 45° to the fibre axes at ΔK_{ini} of 14 MPa$\sqrt{m}$ shows a single dominant crack instead of multiple cracking as found in laminates when tested at ΔK_{ini} of 10 and 12 MPa$\sqrt{m}$. By increasing the load range, crack growth became faster and the specimen failed after only 102,364 cycles. Hence it is deduced that less time was available to initiate other cracks and for their early growth even at this slightly higher ΔK_{ini}. Fig. 4 shows a plot of crack growth rate *vs* crack length of a laminate

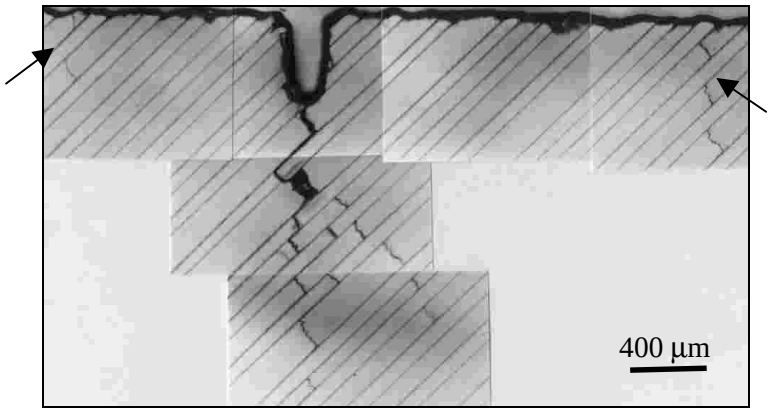

Fig. 3: Micrograph of an acetate replica taken after 440,000 cycles showing the initiation and early growth of two secondary cracks (arrowed) for the laminate with the mode-I crack growth direction at 45° to the fibre axes and at ΔK_{ini} = 12 MPa$\sqrt{m}$.

with the mode-I crack growth direction at 45° to the fibre axes, with an initial notch length (a_0) of 1mm. In this case the CA/CF transition was found to be 10-12 MPa$\sqrt{m}$, which is higher than the CA/CF transition at a_0 = 0.5 mm, but similar to that for the laminates with the mode-I crack growth direction at 30 and 60° to the fibre axes at a_0 = 0.5 mm. By increasing the notch length a lower load was required for the same initial stress intensity factor which raises the CA/CF transition and the fatigue life of the laminate with the mode-I crack growth direction at

45° to the fibre axes. This is consistent with the trends of CA/CF transitions observed in previous work on unidirectionally reinforced Ti MMCs [3]. Fig. 5 shows the single dominant crack obtained for the laminate with the mode-I crack growth direction at 45° to the fibre axes at ΔK_{ini} of 12 MPa$\sqrt{m}$ and for an initial notch length of 1 mm.

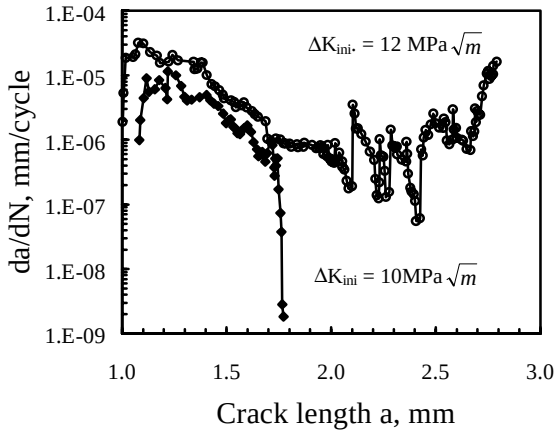

Fig. 4: da/dN versus crack length for the laminate with the mode-I crack growth direction at 45° to the fibre axes, at notch length of 1 mm.

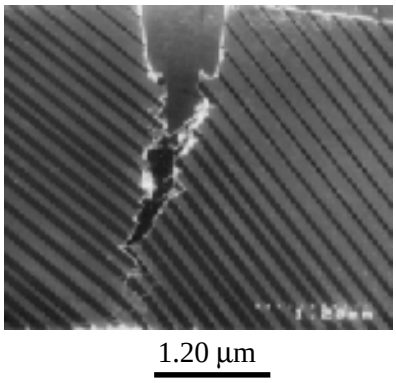

Fig. 5: Fracture surface of the polished specimen with the mode-I crack growth direction at 45° to the fibre axes showing single dominant crack at ΔK_{ini} = 12 MPa$\sqrt{m}$ and a_0 = 1mm.

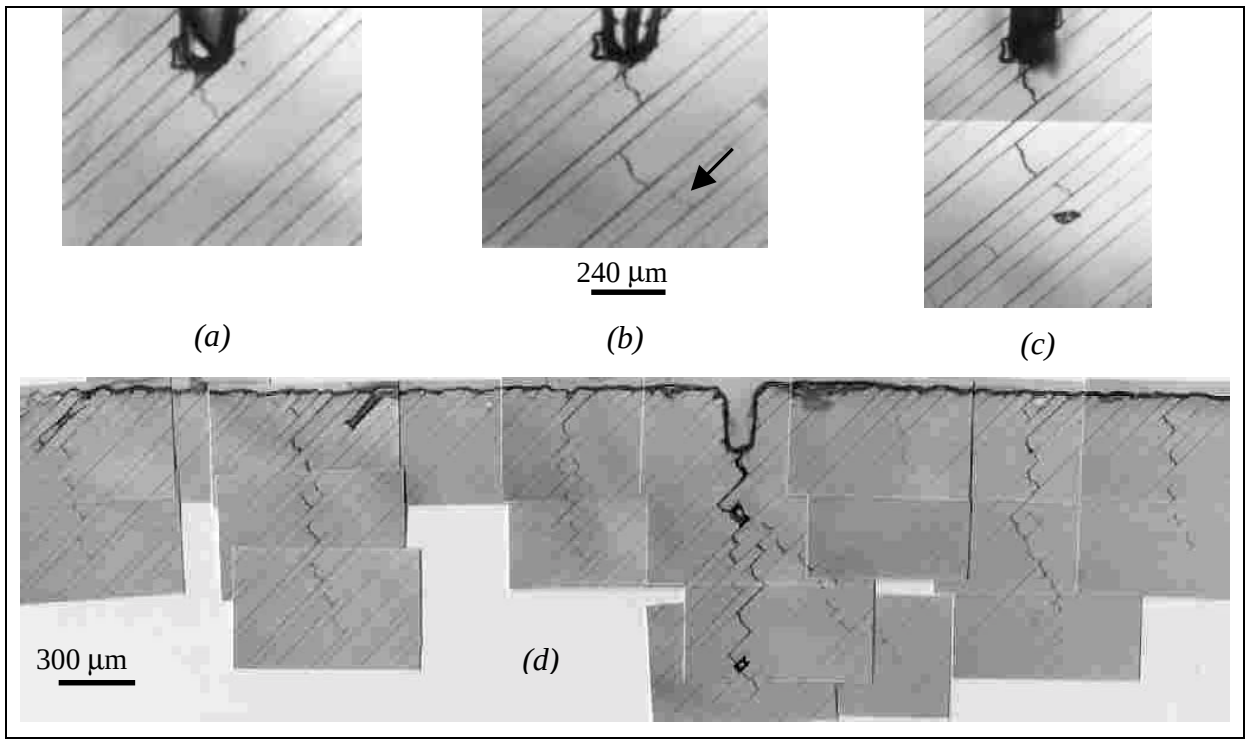

Fig. 6: Micrograph of acetate replicas showing –45 surface layer for the laminate with the mode-I crack growth direction at 45° to the fibre axes, at ΔK_{ini} of 12 MPa√m (a) after 10,000 cycles (b) after 35,000 cycles (c) after 70,000 cycles and (d) after 1,200,000 cycles.

Fig. 6 displays acetate replicas taken during the test, showing the fatigue crack propagation on the -45 layer (surface layer) of the laminate with the mode-I crack growth direction at 45° to the fibre axes, at ΔK_{ini} of 12 MPa$\sqrt{m}$. The primary crack initiates from the notch after extensive interfacial debonding. The first matrix crack first appears at this surface position after 10,000 cycles perpendicular to the fibre as shown in fig. 6.a. After 35,000 cycles the crack deflects to an angle of 45° to the mode-I crack growth direction (Fig. 6.b, arrowed), and the primary crack bifurcates after 70,000 cycles (Fig. 6.c). After 300,000 cycles, the primary crack stops growing while the first secondary crack starts to grow. At the end of the test, a total of six secondary cracks were found on the surface excluding the primary crack. The first fibre failure on the surface was observed after 200,000 cycles. All the fibres surrounding the primary crack failed either at or near to the primary crack plane. A few fibre failures were also observed near to the secondary crack plane. Thus a huge damage zone developed in front of the notch root. With further cycling the primary crack became active again and there were a number of fibre failures near to the primary crack plane leading to rapidly accelerating primary crack growth and final failure of the primary crack along the mode-I direction.

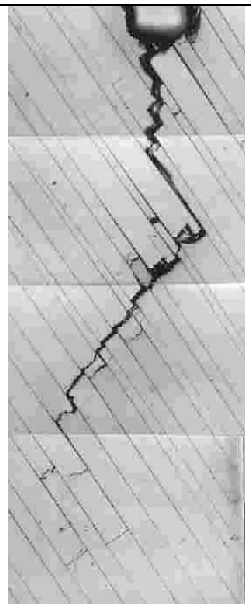

Fig. 7: Micrograph of acetate replica showing 60° surface layer for the laminate with the mode-I crack growth direction at 60° to the fibre axes at ΔK_{ini} of 12 MPa$\sqrt{m}$ after 315,000 cycles.

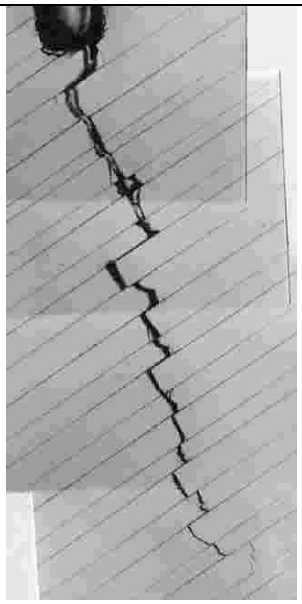

Fig. 8: Micrograph of acetate replica showing 30° surface layer for the laminate with the mode-I crack growth direction at 30° to the fibre axes at ΔK_{ini} of 12 MPa$\sqrt{m}$ after 150,000 cycles.

The crack propagation behaviour on the 60° ply (surface layer) of the laminate with the mode-I crack growth direction at 60° to the fibre axes at ΔK_{ini} of 12 MPa$\sqrt{m}$ just before failure is shown in Fig. 7. As for the laminate with the mode-I crack growth direction at 45° to the fibre axes, a primary crack initiated with interfacial debonding and matrix cracking. The first matrix crack was observed after 15,000 cycles. The primary crack remained along the mode-I crack growth direction for 40,000 cycles, and when it deflected at an angle of 35° from the mode-I direction and started to grow perpendicular to the fibres. The first fibre failure was observed after 30,000 cycles which is earlier than with the laminate with the mode-I crack growth direction at 45° to the fibre axes. This is deduced to be due to an artefact of polishing. Polishing removes some of the first layers of fibres, presumably weakening them. The specimen with the mode-I crack growth direction at 60° to the fibre axes had a greater proportion of the first layer of fibres removed (by chance) than the specimen with the mode-I

crack growth direction at 45° to the fibre axes. After polishing it was found that the specimen with the mode-I crack growth direction at 60° to the fibre axes had had a greater proportion of the fibre removed than the specimen with the mode-I crack growth direction at 45° to the fibre axes. Hence surface fibres were more likely to fail in the specimen with the mode-I crack growth direction at 60° to the fibre axes in these particular tests. All fibre failures were very close to the primary crack and the broken fibres join the separate matrix cracks of the primary crack to make a single dominant crack and eventually the laminate failed catastrophically.

Fatigue crack paths in the laminate with the mode-I crack growth direction at 30° to the fibre axes at ΔK_{ini} of 12 MPa$\sqrt{m}$ display similar behaviour to the laminate with the mode-I crack growth direction at 60° to the fibre axes and is shown in fig. 8. The primary crack initiates by interfacial debonding and fibre failure. The fibre at the notch root was damaged by notching and fails after only 10,000 cycles. The first matrix crack was observed after 15,000 cycles similar to the laminate with the mode-I crack growth direction at 60° to the fibre axes. However unlike the laminate with the mode-I crack growth direction at 60° to the fibre axes, the primary crack starts to deflect perpendicular to the fibre immediately. With continued cycling, there is more matrix cracking and more fibre failure on the primary crack plane to make a single dominant crack at an angle of approximately 30° with the mode-I direction and finally the specimen fails catastrophically along the primary crack plane.

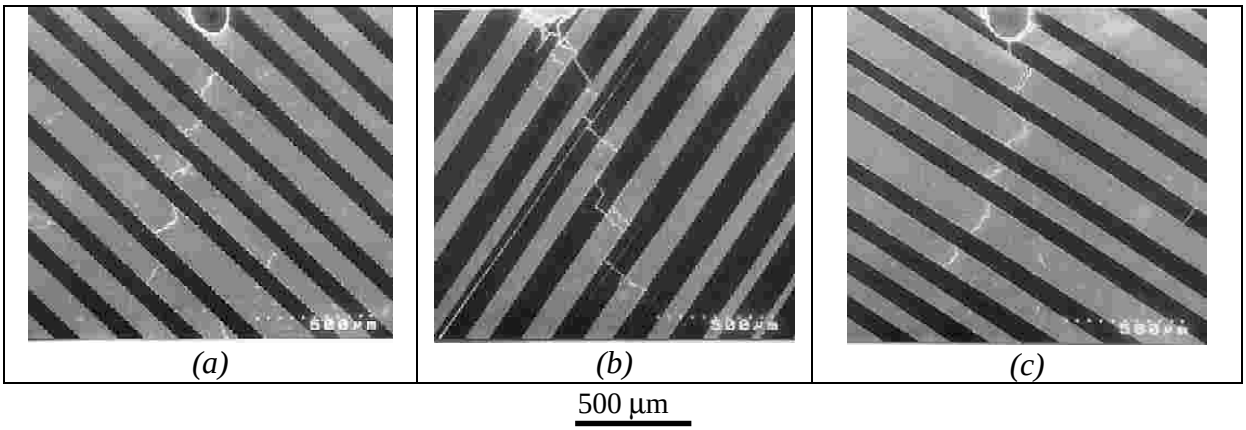

Fig. 9: SEM micrographs of crack arrested specimens showing single dominant cracks with fibre bridging at an angle to the mode-I crack growth direction. Laminates with the mode-I crack growth direction at (a) 45° (b) 60° (c) 30° to the fibre axes respectively.

Fig. 9 shows SEM micrographs of specimens where the fatigue cracks arrested, for the three different angles of crack growth with respect to the fibre axes considered here. Unlike unidirectional composites [3] and $[0/90]_{2s}$ cross-ply laminates [13], a single dominant crack is initiated from the notch at an angle to the mode-I crack growth direction (See Table 2) and

Table 2 : Number of fibre failures in crack arrested specimens.

Laminates with mode-I crack growth direction	ΔK_{ini}, MPa$\sqrt{m}$	No. of fibre failures from AE	No. of fibre failures from acetate replica	Crack angle with mode-I crack growth direction (From fig.9)
45°, polished	8	0	0	16°
60°, polished	10	5	4	20°
30°, polished	10	4	1	30°

each matrix crack is found usually to be perpendicular to the surface fibre direction and (hence) parallel to the direction of the next layer of fibres buried beneath the surface. However, specimens where the crack arrested do show the interfacial debonding, matrix cracking and fibre bridging seen in unidirectional and $[0/90]_{2s}$ and $[90/0]_{2s}$ laminates. Table 2 shows the number of fibre failures in crack arrested laminates detected by acoustic emission (AE) which is very close to the number of fibre failures observed on the surface. The reason for surface fibre failure in the crack arrested specimen of the laminate with the mode-I crack growth direction at 60° to the fibre axes may be that polishing here (by chance) removes almost half of the diameter of some of the fibres in the surface layer and thus makes it more fragile at these surface positions as described earlier.

Fig. 10 shows macrographs of crack profiles revealed by heat tinting crack arrested specimens. It can be seen from this figure that an approximately straight crack profile was obtained through thickness for all three laminates, which is in contrast to observations made on $[0/90]_{2s}$ and $[90/0]_{2s}$ laminates as found in another study [8]. This observation signifies no apparent influence of stacking sequence on the fatigue crack propagation, however, out of plane deviations need to be considered carefully and will be the subject of further study.

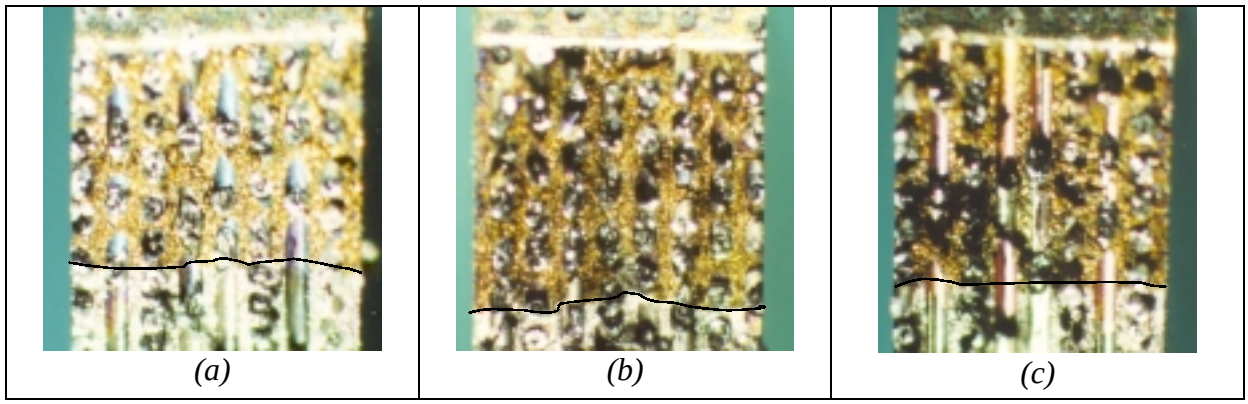

Fig. 10: Fatigue crack profiles of crack arrested specimens revealed by heat tinting treatment. Laminates with the mode-I crack growth direction at (a) 45° (b) 60° (c) 30° to the fibre axes respectively .

From the fatigue behaviour described above, it is clear that this cross-ply laminate with mode-I crack growth direction at 30, 45 and 60° to the fibre axes possess a complicated failure mechanism although they show a similar failure mechanism to that of unidirectional composite or $[0/90]_{2s}$ and $[90/0]_{2s}$ laminates for crack arrested specimens. The laminate with the mode-I crack growth direction at 45° to the fibre axes can show the most complicated behaviour of bifurcation of the primary crack and several through thickness secondary cracks which all grow to almost equal lengths (See fig.6), rather than a single dominant crack as found for laminates with the mode-I crack growth directions at 30 and 60° to the fibre axes (See figs. 7 and 8). This single dominant crack is found always to deflect at an angle with the mode-I axis but grows perpendicular to the first ply fibre direction. The reason for multiple cracks on the surface of polished laminate with the mode-I crack growth direction at 45° to the fibre axes may be the higher number of crack initiation sites which develop by easy interfacial debonding along the 45° fibre direction or that the stress concentration away from the notch tip is still high enough to open the interfaces in the 45° layers [12]. In addition, damage initiation by other fracture mechanisms such as debonding, matrix cracking and fibre failure, and the interaction of these damage mechanisms will further develop a complicated stress

field in front of the notch. However further investigation is required to confirm this mechanism. In spite of such complicated fatigue crack growth behaviour in these laminates, crack arrest is still obtained and is attributed to the intact fibres in the crack wake bridging the crack and thus reducing the effective stress intensity at the crack tip. Hence a deceleration in crack growth rate is obtained [2,3].

The similar CA/CF transition for laminates with the mode-I crack growth directions at 30 and 60° to the fibre axes may be because of equal number of 30 and 60° plies in both these laminates. It is also observed from the heat tinted specimens that both 30 and 60° plies show similar crack profiles. On the other hand, the laminate with the mode-I crack growth direction at 45° to the fibre axes shows a lower CA/CF transition, in spite of having a longer fatigue life than the laminates with the mode-I crack growth direction at 30 and 60° to the fibre axes at ΔK_{ini} of 12 MPa$\sqrt{m}$. Therefore, further investigation is required to elucidate this behaviour but one intriguing possibility is that more fatigue damage can be introduced into fibres at 45° to the mode-I fatigue crack growth direction and hence their in situ fibre strength may degrade further. A detailed investigation of inter-ply damage evolution by monitoring the crack propagation and crack length in each layer of fibres is now also under way to reveal the fatigue mechanism in these laminates in more detail.

CONCLUSIONS

1. The CA/CF transition for the laminate with the mode-I crack growth direction at 45° to the fibre axes is found at ΔK_{ini} of 8-10 MPa$\sqrt{m}$ whereas it is 10-12 MPa$\sqrt{m}$ for laminates with the mode-I crack growth direction at 30 and 60° to the fibre axes at an initial notch length of 0.5 mm. However the laminate with the mode-I crack growth direction at 45° to the fibre axes shows a higher CA/CF transition (10-12 MPa$\sqrt{m}$) at an initial notch length of 1 mm.

2. Crack propagation always occurs at an angle to the mode-I crack growth direction and is usually perpendicular to the fibre axes observed at the surface position.

3. The laminate with the mode-I crack growth direction at 45° to the fibre axes can show more complicated crack propagation behaviour. A single dominant crack is found for both laminates with the mode-I crack growth direction at 30 and 60° to the fibre axes, whereas the laminate with the mode-I crack growth direction at 45° to the fibre axes shows a bifurcated primary crack and can develop multiple secondary cracks.

ACKNOWLEDGEMENTS

One of the authors (A.Y.) would like to acknowledge the financial support from the ORS (CVCP) Committee and the School of Metallurgy and Materials. Another of the authors (T.J.A.D.) has been supported by the EPSRC Foundation Programme within the IRC in Materials for High Performance Applications during the course of this study. Thanks are also due to Rolls-Royce plc., Derby for the provision of material.

REFERENCES

1. Mall, S. and Nicholas, T., *Titanium Matrix Composites-Mechanical Behaviour*, Technomic Publishing Company, Inc., 1998.
2. Ibbotson, A.R., Beevers, C.J and Bowen, P., "Stable and Unstable Crack Growth Transitions Under Cyclic Loading in a Continuous Fibre Reinforced Composite", *Scripta Met.*, Vol. 25, No. 8, 1992, pp. 1781-1786.

3. Bowen, P., "Characterization of Crack Growth Resistance Under Cyclic Loading in the Presence of an Unbridged Defect in Fibre-Reinforced Titanium Metal Matrix Composites", *ASTM STP 1253, ASTM*, 1996, pp. 461-479.

4. Warrier, S.G., Majumdar, B.S. and Miracle, D.B., "Interface Effects on Crack Deflection and Bridging During Fatigue Crack Growth of Titanium Matrix Composites", *Acta Mater.*, Vol. 45, No. 12, 1997, pp. 4969-4980.

5. Covey, S.J., Lerch, B.A. and Jayaraman, N., "Fibre Volume Fraction Effects on Fatigue Crack Growth in SiC/Ti-15-3 Composite", *Materials Science and Engineering*, A200, 1995, pp. 68-77.

6. Lerch, B. and Halford G., "Effect of Control Mode and R Ratio on the Fatigue Behaviour of a Metal Matrix Composite", *Materials Science and Engineering*, A200, 1995, pp. 47-54.

7. Brisset, F. and Bowen, P., "Fatigue Crack Growth in Fibre Reinforced Titanium MMC Laminate at Room and Elevated Temperatures", *Materials Science and Technology*, Vol. 14, 1998, pp. 651-657.

8. Pursell, J.G., Takashima, K. and Bowen., "Effects of Fibre Failure and Fibre Architecture on Fatigue Crack Growth in Notched Titanium Metal Matrix Cross-ply Laminates", *P., Proc. 3rd Japan International SAMPE Symposium*, Vol. 2, 1993, pp. 1818-1823.

9. Boyum, E.A. and Mall, S., "Fatigue Behaviour of a Cross-ply Titanium Matrix Composite Under Tension-Tension and Tension-Compression Cycling", *Materials Science and Engineering*, A200, 1995, pp. 1-11.

10. Kamat, S.V., Hirth, J.P. and Zok, F.W., “Effects of Notch Root Radius on Crack Initiation and Growth Toughness of a Cross-ply Ti-6-4/SiC Composite”, *Acta Mater*., Vol. 44, No. 5, 1996, pp. 1831-1838.

11. Wang, P.C., Jeng, S.M., Chiu, H.-P. and Yang, J.-M., “Damage Evolution of Angle-ply SCS-6/Ti Composites Under Static and Fatigue Loading”, *Journal of Materials Science*, Vol. 30, 1995, pp. 1818-1826.

12. Nguyen, T.-H., Jeng, S.M. and Yang, J.-M., “The Effect of Fibre Orientation on Fatigue Crack Propagation in SCS-6/Ti-15-3 Composites”, *Materials Science and Engineering*, A183, 1994, pp. 1-9.

13. Yasmin, A., Doel, T. J. A. and Bowen, P., “Effects of Fibre Orientation on the Fatigue Crack Growth Resistance of Ti-6Al-4V/SCS-6 Laminates”, *Fatigue, ’99*.